Rapid aqueous photo-polymerization route to polymer and polymer-composite hydrogel 3D inverted colloidal crystal scaffolds

Yuanfang Liu,[1] Shaopeng Wang,[1] Justin Krouse,[1] Nicholas A. Kotov,[2,3,4] Mohammad Eghtedari,[5] Gracie Vargas,[5,6] Massoud Motamedi[5]

[1]*ICx Nomadics, Inc., 1024S Innovation Way, Stillwater, Oklahama 74074*
[2]*Department of Chemical Engineering, University of Michigan, Ann Arbor, Michigan 48109*
[3]*Department of Biomedical Engineering, University of Michigan, Ann Arbor, Michigan 48109*
[4]*Department of Materials Science, University of Michigan, Ann Arbor, Michigan 48109*
[5]*Center for Biomedical Engineering, University of Texas Medical Branch, Galveston, Texas 77555*
[6]*Department of Neuroscience and Cell Biology, University of Texas Medical Branch, Galveston, Texas 77555*

Received 21 July 2005; revised 26 October 2006; accepted 29 November 2006
Published online 2 March 2007 in Wiley InterScience (www.interscience.wiley.com). DOI: 10.1002/jbm.a.31199

Abstract: Successful regeneration of biological tissues *in vitro* requires the utilization of three-dimensional (3D) scaffolds that provide a near natural microenvironment for progenitor cells to grow, interact, replicate, and differentiate to form target tissues. In this work, a rapid aqueous photo-polymerization route was developed toward the fabrication of a variety of polymer hydrogel 3D inverted colloidal crystal (ICC) scaffolds having different physical and chemical properties. To demonstrate the versatility of this technique, a variety of polymer hydrogel ICC scaffolds were prepared, including (1) polyacrylamide (pAAM) scaffolds, (2) poly(2-hydroxyethyl methacrylate) (pHEMA) scaffolds, (3) poly(2-hydroxyethyl acrylate) (pHEA) scaffolds, and composite scaffolds including (4) pAAM-pHEMA scaffolds, (5) pHEMA-pMAETAC [poly(2-methacryloyloxy) trimethyl ammonium] scaffolds, and (6) pHEA-pMEATAC scaffolds. Templates for scaffolds incorporated both uniform sized (104 μm diameter) and nonuniform sized (100 ± 20 μm diameter) closely packed noncrosslinked poly(methyl methacrylate) beads. Human bone marrow stromal HS-5 cells were cultured on the six different types of scaffolds to demonstrate biocompatibility. Experimental results show that cells can remain viable in these scaffolds for at least 5 weeks. Of the six scaffolds, maximal cell adhesion and proliferation are obtained on the positively charged composite hydrogel pHEMA-pMEATAC and pHEA-pMAETAC scaffolds. © 2007 Wiley Periodicals, Inc. J Biomed Mater Res 83A: 1–9, 2007

Key words: inverted colloidal crystal; hydrogel scaffold; photo-polymerization; HS-5 human bone marrow stromal cells; three-dimensional (3D)

INTRODUCTION

Cell scaffolds play an important role in tissue engineering by providing a near natural microenvironment for growing cells.[1] An ideal scaffold is one that possesses physical and chemical properties similar to natural tissues and does not induce immunologic host response.[2] In addition, the scaffold should provide cells with sufficient nutrients and oxygen, remove their waste products, and allow the cells to adhere, migrate, and interact with each other just like they do in their natural environment.[3] The material property and surface nature of the scaffolds affect cell attachment, proliferation, differentiation, and ultimately new tissue regeneration.

Synthetic polymer hydrogels are three-dimensional (3D) macromolecular networks that contain a large fraction of water within their structure. They do not dissolve, are soft and pliable, and do not elicit host immune response.[4] These properties are desired to mimic native tissue; therefore, hydrogels are particularly useful in biomedical and pharmaceutical applications.[5,6] Hydrogel polymers are particularly appealing candidates for the design of highly functional tissue engineering scaffolds.[7–9] The intrinsic

Correspondence to: S. Wang; e-mail: swang@nomadics.com

Contract grant sponsor: DARPA; contract grant numbers: DAMD17-02-1-0702, W81XWH-04-C-0139
Contract grant sponsor: Oklahoma Center for the Advancement of Science and Technology; contract grant number: AR 03 (2)-068

elasticity and wear retention ability of synthetic hydrogels resemble those of natural hydrogels such as collagen matrices, which are prevalent as structural scaffolds in various connective tissues including bone.[4] The porosity of synthetic hydrogel scaffolds and other scaffolds may be controlled by various techniques including solvent casting/particulate leaching,[10,11] phase separation,[12] gas foaming,[13] solvent evaporation,[14] freeze-drying,[15] blending with a noncrosslinkable linear polymer,[16] and polymer colloidal crystal template technique.[17,18] These techniques afford a range of mechanical and structural properties. Another important feature of hydrogels is that they can be assembled in 3D form, displaying multiple functional domains through copolymerization of different monomers. The polymerization chemistry of hydrogels is water compatible. This allows the incorporation of polar ligands, such as aniopeptides, that mimic the acidic matrix proteins regulating mineral growth and biological epitopes such as the tripeptide RGD,[19–21] which promote cellular adhesion. Still another advantage of hydrogel scaffolds is their relative transparency, which allows for noninvasive imaging of growing cells in thick scaffolds using high resolution microscopy such as confocal or two-photon microscopy.

Polyacrylamide (pAAM), poly(2-hydroxyethyl methacrylate) (pHEMA), poly(2-hydroxyethyl acrylate) (pHEA), and poly(2-methacryloyloxy) trimethyl ammonium (pMAETAC) are known synthetic hydrogel polymers.[7,18,22,23] Usually, these polymer hydrogels are synthesized by thermal polymerization including solution polymerization and inverse suspension polymerization.[7,18,22–25] Photo polymerization is a common method used to synthesize polymers. This method has been used in the preparation of polymer hydrogels for tissue engineering applications[26–29] including the synthesis of poly (ethylene glycol) 3D cell scaffolds.[29] The rapid preparation of cell scaffolds that can support accelerated cell proliferation and differentiation is very important for rapid tissue regeneration and wound healing. Photo-polymerization, compared with other polymerization methods such as thermal polymerization, has many advantages. These include short reaction times, simple reaction routes, room temperature reactions, biocompatibility, and it is environmentally friendly.[30]

In this work, a rapid photo-polymerization route was developed toward the preparation of polymer hydrogel cell scaffolds having a variety of chemical and physical properties. The versatility of this technique was demonstrated by preparing different component polymeric scaffolds including PAAM, pHEMA, pHEA polymer hydrogel inverted colloidal crystal (ICC) scaffolds, pAAM-pHEMA, pAAM-pMAETAC, pHEMA-pMEATAC, and pHEA-pMAETAC copolymer hydrogel ICC scaffolds. Noncrosslinked PMMA beads of uniform size (104 μm diameter) and nonuniform size (104 ± 20 μm diameter) configured into close-packed assemblies were used as templates to control the porosity of the scaffolds. The structures of the scaffolds were inspected by scanning electron microscopy (SEM) and confocal microscopy. HS-5 human bone stromal cells were cultured in the scaffolds to demonstrate their biocompatibility and to compare the cell adhesion and proliferation rate in different formulated scaffolds. Copolymer hydrogel scaffolds containing positively charged pMAETACC showed markedly improved cell adhesion and proliferation on HS-5 cell culture over scaffolds that did not contain positively charged pMAETACC.

EXPERIMENTAL SECTIONS

Materials

Acrylamide (AAM), *N-N′*-methylene-bisacrylamide (NMBA), 2-hydroxyethyl methacrylate (HEMA), 2-hydroxyethyl acrylate (HEA), ethylene glycol dimethacrylate (EGDA), (2-methacryloyloxy) trimethyl ammonium (MEATAC) ethylene glycol, tetrahydrofuran (THF), and noncrosslinked poly(-methyl methacrylate) (PMMA) were obtained from Sigma. PMMA (104 μm) was obtained from Microparticles, GMBH was from Berlin, Irgacure 819 was from Ciba Specialty Chemicals, and FITC (fluorescein isomer) was from VWR.

The preparation of scaffolds

The preparation of ordered colloidal crystals and nonordered bead array

Preparation of 104 μm PMMA colloidal crystal template

The preparation of colloidal crystals is according to the previous reports.[17,18] Briefly, 1 mL of ethanol was added to 0.1 g of 104 μm PMMA beads. The mixture was sonicated for several minutes until an unstable but uniform dispersion was made. Then, the vial with the mixture was shaken gently for 1 h by ultrasonic force and the PMMA spheres self-assembled into a colloidal crystal. An aliquot of ethanol was withdrawn and the remaining ethanol was allowed to evaporate for 1–2 days. The resulting colloidal crystal arrays were heated at 120°C for 24 h to anneal the particles.

Preparation of nonordered bead-array

Briefly, 1.5 g of PMMA microspheres with a size of 100 ± 20 μm were filled into glass vials measuring 0.35 mm in diameter and 3 cm in height. The vials were glued on a glass dish and then were gently shaken for 1 h with an ultrasonic cleaner to allow the PMMA spheres to assemble into a close-packed structure. The resulting bead-arrays

were heated at 120°C for 24 h to anneal the particles. These cylindrical bead-arrays were used as a template to produce master scaffolds that were then cut into pieces that matched regular sized scaffolds.

The preparation of ordered and nonordered ICC scaffolds

1. The preparation of AAM monomer solution: 0.2 mL of 5% NMBA solution was added to 1 mL of 30% of acrylamide to form a uniform mixture solution. Approximately, 1 mg of IRG819 powder was added to the mixture solution.
2. The preparation of HEMA monomer solution:4 mL of HEMA monomer, 1 mL of water, 4 drops of ethyl glycol dimethacrylate (EGDA), and approximately 1 mg of Irgacure 819 were mixed to form a HEMA mixture solution.
3. The preparation of HEA monomer solution: 2 mL of HEM, 0.5 mL of distilled water, 2 drops of ethyl glycol dimethacrylate (EGDA), and approximately 1 mg of Irg819 were mixed to form a HEA mixture solution.
4. The preparation of AAM-HEMA monomer solution: 4 mL of HEMA monomer, 1 mL of water, 4 drops of ethyl glycol dimethacrylate, and approximately 1 mg of Irgacure 819 were mixed to form solution I. 1 mL of 30% AAM (acrylamide) solution, 0.2 mL of 5% NMBA solution, and 1 mg of Irg819 were mixed to obtain solution II. A 1:5 volume ratio of solution I and solution II were mixed to form AAM-HEMA mixture solution.
5. The preparation of HEMA-MEATAC monomer solution: 0.5 mL of HEMA mixture solution and 50 μL of MEATAC were mixed to obtain a HEMA-MEATAC mixture solution.
6. The preparation of HEA-MEATAC monomer solution: 1 mL of HEA, 0.25 mL of H_2O, 50 μL of MEATAC, 1 drop of EDTA, and 1 mg of IRG819 were mixed to form a HEA-MEATAC mixture solution.
7. The preparation of scaffolds: These 6 types of monomer precursor solutions were infiltrated into the PAAM uniform sized colloidal crystals and the nonuniform sized PMMA arrays, respectively. The composite of beads and monomer solution was then photo-polymerized under 365 nm of UV light for different times. The resulting gel composite and PMMA spheres was soaked in THF to remove the PMMA microspheres for 3 days and then was soaked in water for 1 h. The polymer and copolymer scaffolds were then obtained.

The rod-like scaffolds with nonuniform pores/cavities can be produced on a large-quantity scale. Ten rod-like master scaffolds with different types of polymers have been produced in one batch. Each rod-like scaffold can be cut into 20–25 round-disk shaped scaffolds with a diameter of 3.5 mm and a thickness of 1 mm. Therefore, 200–250 scaffolds can be fabricated in one batch from 10 master scaffolds. Larger batches can be produced by making additional master scaffolds.

Cell culture

HS-5 human bone marrow stromal cells were obtained from ATCC (CRL-11882). An ATCC recommended medium was used to culture the cells that included: Dulbecco's modified Eagle's medium with 4 m*M* L-glutamine, 4.5 g/L glucose, 1.5 g/L sodium bicarbonate (ATTC 30-2002) supplemented with 10% fetal bovine serum (ATCC 30-2021), and 1% penicillin–streptomycin (Sigma P3539). Scaffolds were placed in either a 96 or 48 well nontissue-culture-treated microplate seeded with 10^4–10^5 cells per well with a 0.2–0.5 mL medium and incubated at 37°C with 5% CO_2. The medium was changed every 1–3 days.

Characteristics of scaffolds and cells

The characteristics of scaffold structure and cultured cells were investigated by scanning electronic microscopy (SEM) and confocal microscopy.

SEM images were obtained with a JSM 6400 microscope. Scaffold samples for SEM were first dried in air naturally and then coated with a thin conductive film of gold using a Denton Desktop III sputter.

Confocal microscopy images were obtained with a Leica SP2 confocal microscope. To observe scaffold structures, the scaffold was coated with FITC to reveal the structure (excitation wavelength is 488 nm; emission detection band is 500–550 nm). To observe the cells on the scaffold, the cells were stained with a live/dead viability staining kit from Invitrogen (L-3224). This procedure was performed as follows: the cells were washed with a serum free medium and stained with a serum free medium containing 0.5 μ*M* calcein AM and 0.5 μ*M* ethidium homodimer-1 (ETH) for 30 min at 37°C. The cells were then washed with a serum free medium one more time and replaced with a regular medium then incubated for 1 h prior to imaging. Confocal microscopy excitation wavelengths were 488 nm and 543 nm with a laser for the calcein (green, live cells) and ETH labels (red, apoptotic cells) with emissions detected by using 500–535 nm and 600–650 nm bandpass filters, respectively. For each interested area of the sample, 30 stacked images across 150 μm depth were obtained and the projection images of the maximum intensity of the stacked images presented.

Two photon laser scanning microscopy was performed using a Zeiss LSM410 confocal microscope equipped with a tunable Ti: Sapph femtosecond laser running at a 82 MHz repetition rate and a 100 femtosecond pulse width (Tsunami, Spectra Physics). The average power measured at the objective entrance was 50 mW. To image calcein-stained cells, the excitation source was tuned to 760 nm and the fluorescence emission was collected at 500–540 nm. A 40×, 0.8 N.A. long working distance objective lens was used to capture 50 Z-section images with a step of 2 μm. ImageJ software was used to generate z-projection images from z-stacks.

Quantitative assessment of the scaffold to accommodate human stromal bone marrow cells: Five disk-shape scaffolds with a diameter of 5 mm and a thickness of 1 mm each made from the different polymers described above

were placed in five wells on a 12-well culture plate, and 1 mL of complete culture media (DMEM supplemented with 10% fetal bovine serum) was added to engulf the scaffolds. A 50 μL cell pellet containing 10^5 human stromal bone marrow cells (HS-5) was placed on top of each scaffold and the plate was incubated at 37°C in the presence of 5% CO_2 to allow cells to adhere and proliferate within scaffolds. After 48 h, live cells on the scaffolds were stained using calcein-AM fluorescent dye and two-photon microscopy was performed to determine the number of live cells in the most crowded area of each scaffold.

RESULTS AND DISCUSSION

The structure of colloidal crystals and scaffolds

To obtain templates that have adequate mechanical strength for making scaffolds, it is particularly important to anneal PMMA colloidal crystals and the PMMA close-packed array at 120°C for 24 h before the hydrogel solution is infiltrated into them. The annealing makes the beads stick to each other, which (1) enhances the mechanical strength of the crystal and the template, (2) enlarges the connected area of the beads through effective solvent casting and complete dissolving of the beads after the scaffold were polymerized, and (3) allows the formation of larger interconnection channels (30–50% in diameter of the cavity size) between the inverted opals of the scaffold, which is important for cell migration and nutrient transport.

The pHEMA scaffold is selected as a representative to show the structure of the scaffolds from a 104 μm PMMA colloidal crystal template. For SEM, pHEMA scaffolds were air dried. SEM micrographs of the free surface of pHEMA scaffolds are shown in Figure 1. The insert in Figure 1 is a SEM micrograph of a colloidal crystal template. The PMMA beads are assembled into an ordered structure. The size of the beads is 102 μm, which did not change significantly compared with the original size of 104 μm. The cavity

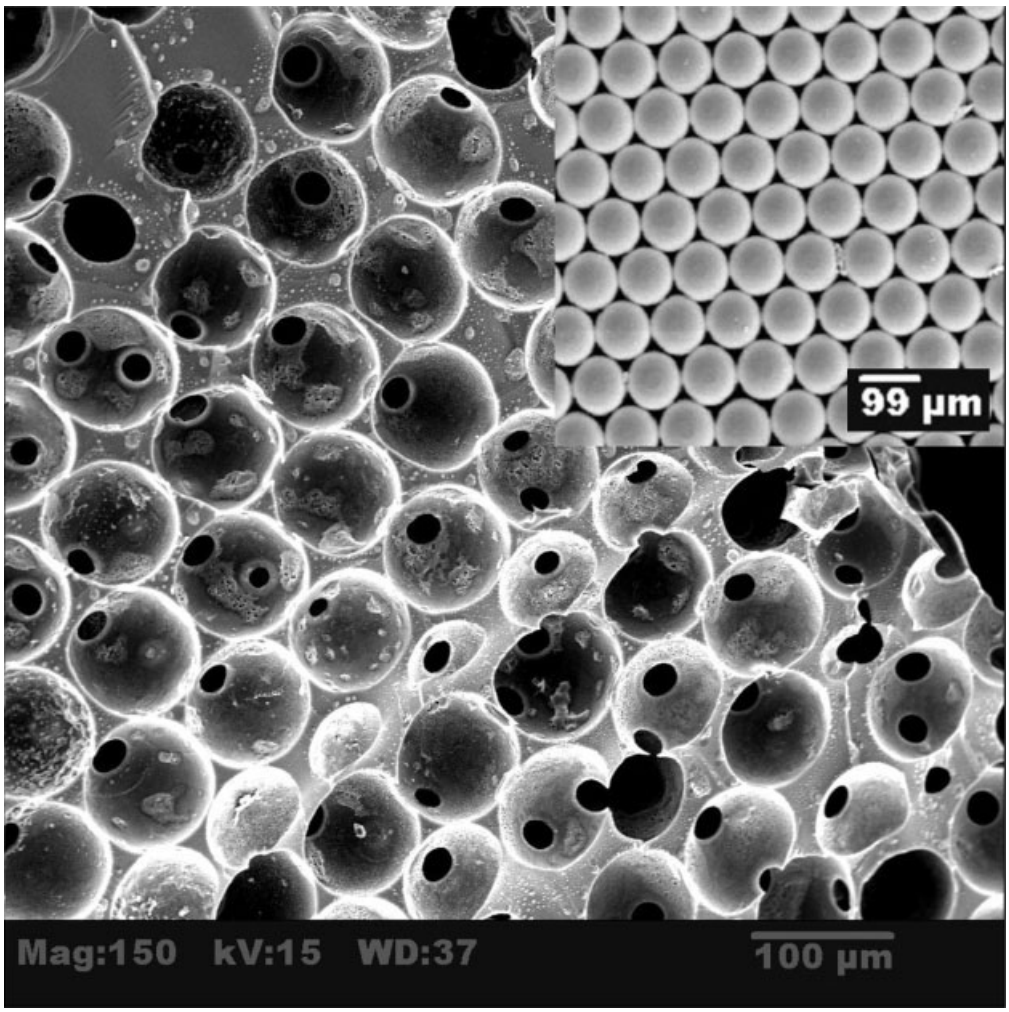

Figure 1. SEM images of the free surface of a pHEMA scaffold and the corresponding 104 μm colloidal crystals template (insert).

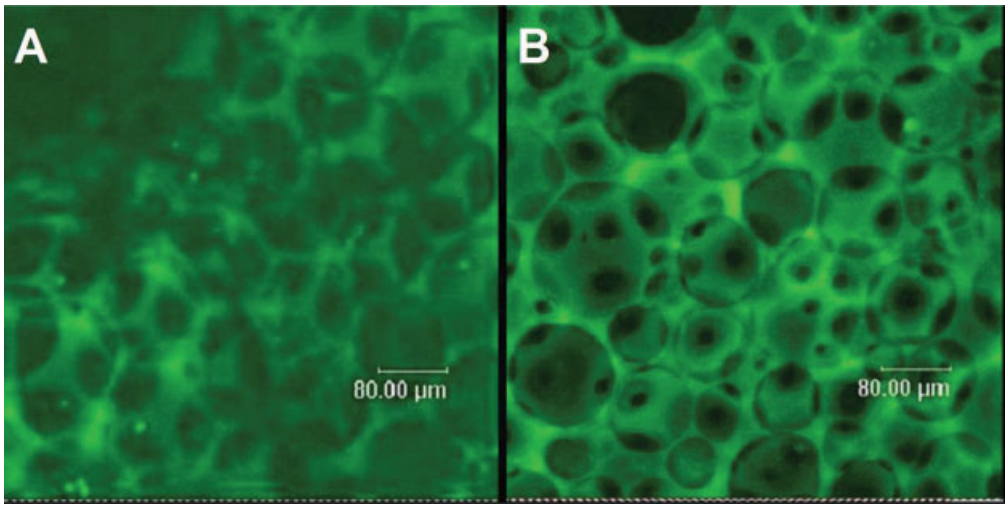

Figure 2. Confocal images of (A) ordered and (B) nonordered pHEMA scaffolds. [Color figure can be viewed in the online issue, which is available at www.interscience.wiley.com.]

size of the scaffold is about 90 μm (Fig. 1); however, this is smaller than the bead size of 104 μm. This is attributed to hydrogel scaffolds shrinking during the dehydration process for SEM sample preparation. Accordingly, the interconnection channels are about 20 μm and on the order of the size of the cell, which should be sufficient for cell migration through the interconnecting passages of the 3D scaffold.

Figure 2(A) is the confocal image of the FITC-coated pHEMA scaffolds made from a 104 μm PMMA template and Figure 2(B) is the confocal image of FITC-coated pHEMA scaffolds made from nonuniform sized PMMA bead (100 ± 20 μm) assembled template. The image in Figure 2(A) clearly shows the ordered scaffold retains the ICC structure of the PMMA colloidal crystal template. The cavity size is ~125 μm, which is larger than the diameter (104 μm) of the spheres in the PMMA colloidal crystal because the hydrogel expands in volume when placed in aqueous solution. The diameter of the connection channel is about 30–35 μm. For the nonordered scaffold [Fig. 2(B)], the cavity size varies from 50–150 μm and the connection channel is 15–30 μm, which is smaller than that in the ordered scaffolds. The cavity sizes of the scaffolds are comparable with the pore size of nature bone marrow.[31]

The difference between the ordered and nonordered scaffolds is that the ordered scaffolds have same sized porosities and connection channels but those in the nonordered scaffolds vary considerably. The highly ordered structure makes it possible for computer modeling of the nutrient flux, metabolism, cell migration, and other processes on the scaffold, which is difficult on disordered 3D scaffolds. However, this latter structure is similar to native bone marrow, which is also highly nonordered. We expect cells to grow regardless of the order of the scaffold as long as the scaffold has proper sized cavities and connection channels.

The structure of the different hydrogel scaffolds made from nonuniform PMMA bead templates by large-scale production is shown in Figure 3. The maximum and minimum size of the cavities and connection channels of different scaffolds were measured from the corresponding confocal images in Figure 3 and summarized in Table I. The positively charged pAAM-pMEATAC and pHEA-pMEATAC scaffolds [Figs. 3(E,F)] swells considerably in water, resulting in a much larger cavities and connection channels. The swelling is attributed to the electrostatic repulsion between the positively charged pMEATAC. When placed into PBS buffer or cell culture media, the positively charged scaffolds shrank to normal size similar to the noncharged scaffolds because the anions in the buffer and/or media neutralized the positive charges on the scaffolds.

The photo-polymerization of polymer hydrogel scaffolds

As mentioned earlier, photo-polymerization of polymer hydrogels have many advantages over the radical thermal polymerization. Most of the polymer hydrogel scaffolds were prepared by radical thermal polymerization. Kotov and coworkers[18] prepared pAAM scaffolds by thermo-initiation polymerization at 70°C for 12 h and redox-initiation polymerization at room temperature for 12 h under a degassed solution by nitrogen. Schneider and coworkers[19] prepared pHEMA-pMEATAC hydrogel scaffolds with fixed charge densities of −200, 0, and +200 m*M* at room temperature. Song et al.[6] developed an approach to pHEMA-Ca_3 $(PO_4)_2$ scaffold mineralization by a room temperature radical technique that

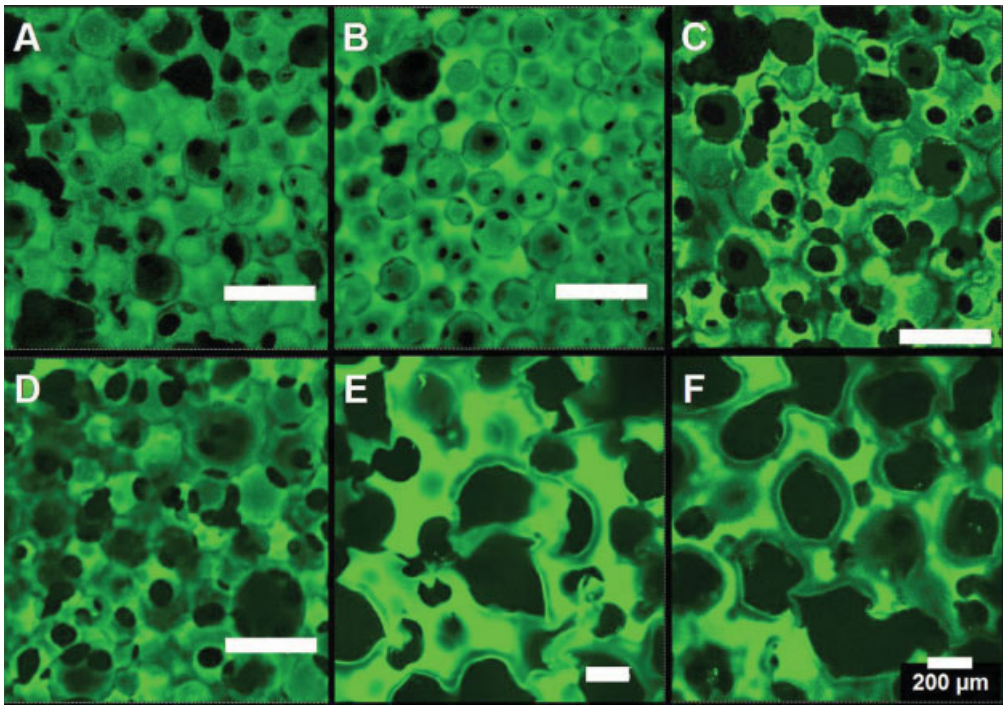

Figure 3. Confocal images of nonordered hydrogel polymer scaffolds: (A) pAAM, (B) pHEMA, (C) pHEA, (D) pAAM-pHEMA, (E) pHEMA-pMEATAC, and (F) pHEA-pMEATAC. [Color figure can be viewed in the online issue, which is available at www.interscience.wiley.com.]

uses an ethylene glycol solution and metabisulfite solution for 12 h. For PAAM, pHEMA, pHEA, pMMA-pHEMA, pHEMA-pMEATAC, and pHEA-pMEATAC polymer hydrogel scaffolds, no photo-polymerization routes were reported except for the preparation of pHEA. Pradas et al.[22] prepared a porous pHEA hydrogel with photo-polymerization for 24 h by using a HEA monomer, EGDMA (ethyleneglycol dimethacrylate) cross-linked agent, and benzoin photoinitiator.

The experimental conditions and results on our scaffold preparation are listed in Table II. The reaction medium is water, and the reaction time is very short. For pAAM polymer hydrogel scaffolds, only 30 min is needed. For pHEMA, pAAM-pHEMA, and pHEMA-pMEATAC polymer scaffolds, it takes 1 h. For pHEA and pHEA-pMEATAC polymer hydrogel scaffolds, it takes 4 and 2 h, respectively. The strength of these scaffolds is strong enough to handle during cell culture and other tests. The appearance of these scaffolds is colorless, semitransparent, or transparent. The scaffolds are sponge like with good elasticity.

The amount of crosslinking agents NMBA and EGTA and the photo-polymerization time have an obvious effect on the hardness and strength of the scaffolds. The hardness and elasticity of the scaffolds were quantified by using tweezers to press the gel and then observing the compressibility. The hardness increases with increases in the NMBA or EGTA amount and reaction time. The proper amount of NMBA, EGTA, and reaction time are shown in Table II. The mechanical strength of all the scaffolds is strong enough for normal handling and cell culture.

Cell culture

Human bone marrow HS-5 stromal cells were cultured on the various scaffolds and cell viability was inspected with a viability kit. Figure 4 shows confocal images of HS-5 stromal cells cultured on different

TABLE I
Cavity and Connection Channel Dimensions of the Nonordered Polymer Inverted Opal Scaffolds

Type of Hydrogel Scaffold	Range of Cavity Diameter (μm)	Range of Connection Channel Diameter (μm)
pAAM	100–140	15–30
pHEMA	50–150	15–30
pHEA	80–120	30–60
pAAM-pHEMA	80–180	40–80
pAAM-pMEATAC (in water)	250–750	100–200
pAAM-pMEATAC (in media)	100–200	20–40
pHEA-pMEATAC (in water)	200–500	30–60
pHEA-pMEATAC (in media)	100–200	15–30

TABLE II
Reaction Conditions and Results of Polymer Inverted Opal Scaffolds

Scaffolds Types	pAAM	pHEMA	pHEA	pAAM-pHEMA	pHEMA-pMEATAC	pHEA-pMEATAC
Monomers	AAM	HEMA	HEA	3:2 (g/g) AAM and HEMA	8:1 (g/g) HEMA and MEATAC	30:1 (g/g) HEA and MEATAC
Cross-linking agents	NMBA	EGTA	EGTA	EGTA	EGTA	EGTA
Photo initiators	Irg819	Irg819	Irg819	Irg819	Irg819	Irg819
Weight ratios of monomer, cross-linking agent and photo initiators	300:10:1	4000:200:1	3000:200:1	5000:3200:200:1	4000:500:200:1	3000:100:200:1
Reaction medium	DH_2O	DH_2O	DH_2O	DH_2O	DH_2O	DH_2O
Reaction time (h)	0.5	1	4	1	1	2
Appearance of scaffolds	Semitransparent	Semitransparent	Transparent	Semitransparent	Transparent	Transparent

formulated hydrogel scaffolds. Cells were stained with 1 μ*M* calcein/ETH stain after 5 days of culture. Green colors are calcein-stained viable cells and red colors are ETH-stained cells that were dead or under apoptosis. The images are maximum intensity projection images of 30 sections over a 160 μm depth. Cells are viable on all scaffolds since most cells are stained by calcein showing green colors and very few were stained with ETH showing red colors. Cells form high-density colonies within the inverted opal are in the following scaffolds: pAAM [Fig. 4(A)], pHEMA [Fig. 4(B)], pHEA [Fig. 4(C)], and pAAM-pHEMA [Fig. 4(D)]. This indicates that (1) cells do proliferate and remain viable in the microenvironment (the cavity) of the inverted opal structure and (2) cells do not adhere well to the scaffold surface. The latter is expected since these scaffolds are hydrophilic and neutral hydrogels have conditions that are not favorable for cell attachment. In contrast, scaffolds doped with positively charged components (pHEMA-pMEATAC, pHEA-pMEATAC) contained cells that spread over the entire surface. Additional cells displayed an elongated morphology along the hydrogel walls as shown in Figures 4(E,F), with rep-

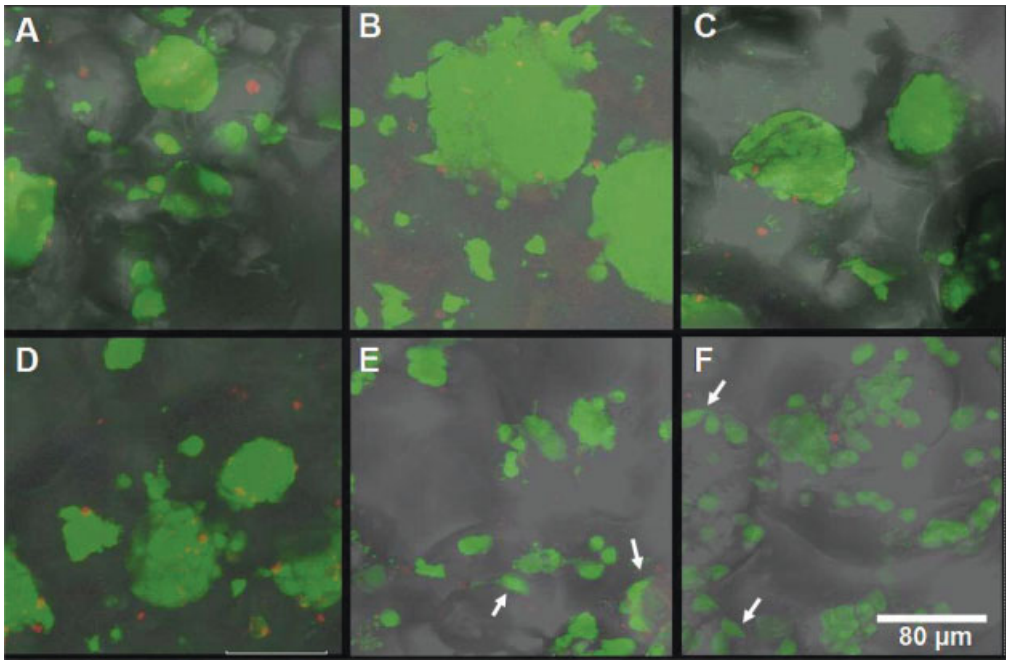

Figure 4. Confocal images of HS-5 human bone marrow stromal cells cultured in non-ordered scaffolds: (A) PAAM, (B) pHEMA, (C) pHEA, (D) pAAM-pHEMA, (E) pHEMA-pMEATAC, and (F) pHEA-pMEATAC. Cells were stained with the viability kit. Green colors are viable cells and red colors are dead cells or cells under apoptosis. [Color figure can be viewed in the online issue, which is available at www.interscience.wiley.com.]

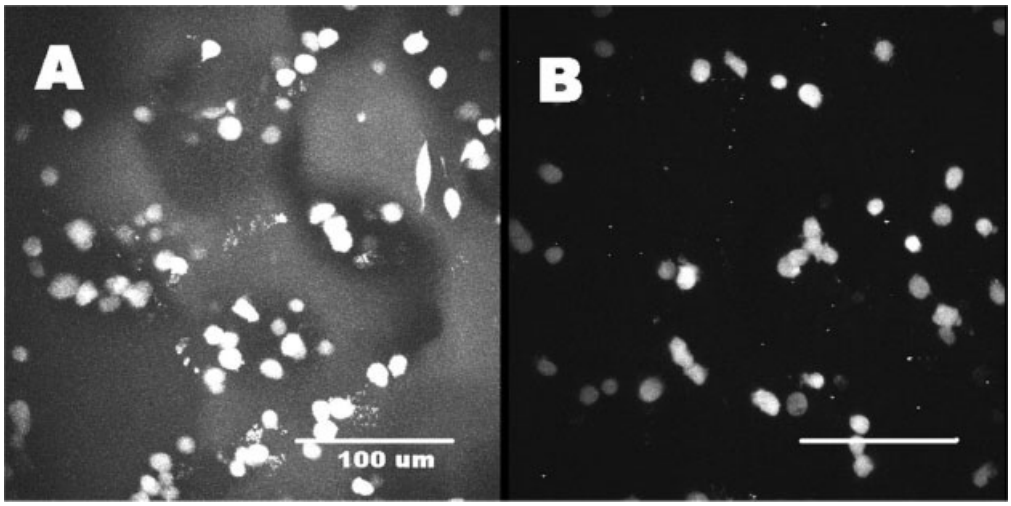

Figure 5. Two-photon microscopic images of HS-5 stromal cells cultured in (A) nonordered pHEMA-pMEATAC scaffolds (depth of imaging = 400 μm) and (B) nonordered pHEMA scaffolds (depth of imaging =160 μm). Scale bar = 100 μm.

resentative cells pointed with the white arrow. This indicates that the positively charged scaffold surface has better cell adhesion than the nonpositively charged surfaces, which is in agree with Schneider's work.[23] The finding of improved cell adherence on a positively charged surface was also noted in cells cultured on the inorganic scaffold that was previously reported.[17]

Two-photon images (Fig. 5) revealed that HS-5 cells can be found to grow as deep as 400 μm inside the nonordered scaffold, similar to that of the ordered scaffold.[17,18] We do not know whether the cells inside the scaffold were initially seeded at that depth or migrated there after seeding. The cells were healthy and growing at this depth, which means that (1) the interconnection channels of the scaffold are large enough to allow the cells to move into the scaffold and (2) there is enough nutrient and oxygen supply at this depth of the scaffold to support cell growth. Therefore, the pore size and interconnection channels of the scaffold are suitable for 3D cell growth and nutrient transportation. The cell density deep inside the scaffold was lower than the surface of the scaffold. This is most likely due to limited nutrient supply as the rapid cell growth at the surface of the scaffold consumed most of the nutrients. This is in agreement with the reported cell distribution of inorganic ICC scaffolds and computational modeling prediction.[32]

Under the same seeding and culture conditions, the number of live HS-5 cells found in the positive-charged scaffold is almost double than that of the neutral-charged scaffold. In a volume of 320 × 320 × 100 μm^3 of pHEMA-pMEATAC and the pHEMA scaffold, 67 and 37 calcein stained live cells were counted, respectively, from the two-photon microscopy 48 h after seeding and incubation at 37°C in the presence of 5% CO_2. This result indicates that the surface of the positively charged scaffold favors cell adhesion and is consistent with the findings from Schneider et al.[23]

CONCLUSION

We demonstrated a rapid aqueous photo-polymerization route to synthesis polymer and polymer-composite hydrogel 3D ICC scaffolds using closely packed noncrosslinked poly(methyl methacrylate) (PMMA) beads with an approximate diameter of 100 μm as a template. This synthetic route is simple, fast, biocompatible, environmental friendly, and versatile. The 3D scaffolds support HS-5 human bone marrow stromal cell adhesion and proliferation deep within the structure. Composite scaffolds with positively charged components were found to have improved cell adhesion and proliferation. These scaffolds have great potential for accelerating *in-vitro* cell culture and *in-vivo* tissue regeneration.

References

1. Hutmacher DW. Scaffold design and fabrication technologies for engineering tissues—State of the art and future perspectives. J Biomater Sci Polym Ed 2001;12:107–124.
2. Jockenhoevel S, Zund G, Hoerstrup SP, Chalabi K, Sachweh JS, Demircan L, Messmer BJ, Turina M. Fibrin gel-advantages of a new scaffold in cardiovascular tissue engineering. Eur J Cardiothorac Surg 2001;19:424–430.
3. Tsang VL, Bhatia SN. Three-dimensional tissue fabrication. Adv Drug Deliv Rev 2004;56:1635–1647.
4. Bakshi A, Fisher O, Dagci T, Himes BT, Fischer I, Lowman A. Mechanically engineered hydrogel scaffolds for axonal growth and angiogenesis after transplantation in spinal cord injury. J Neurosurg Spine 2004;1:322–329.
5. Huang G, Gao J, Hu ZB, John JVS, Ponder BC, Moro D. Controlled drug release from hydrogel nanoparticle networks. J control Release 2004;94:303–311.

6. Peppas NA, Langer R. New challenges in biomaterials. Science 1994;263:1715–1720.
7. Song J, Saiz E, Bertozzi CR. A new approach to mineralization of biocompatible hydrogel scaffolds: An efficient process toward 3-dimensional bonelike composites. J Am Chem Soc 2003;125:1236–1243.
8. Peppas NA. Hydrogels in Medicine and Pharmacy, Vol. 1. Fundamentals. Boca Raton, FL: CRC Press; 1986.
9. Lee KY, Mooney DJ. Hydrogels for tissue engineering. Chem Rev 2001;101:1869–1879.
10. Holy CE, Shoichet MS, Davies JE. Engineering three-dimensional bone tissue in vitro using biodegradable scaffolds: Investigating initial cell-seeding density and culture period. J Biomed Mater Res 2000;51:376–382.
11. Mooney DJ, Cima L, Langer R, Johnson L, Hansen LK, Ingber DE, Vacanti JP. Principles of tissue engineering and reconstruction using polymer-cell construct. Mater Res Soc Symp Proc 1992;252:345–352.
12. Klawitter JJ, Hulbert SF. Application of porous ceramics for the attachment of load bearing internal orthopedic applications. J Biomed Mater Res Symp 1971;2:161–229.
13. Harris LD, Kim BS, Mooney DJ. Open pore biodegradable matrices formed with gas foaming. J Biomed. Mater Res 1998; 42:396–402.
14. Mikos AG, Sarakinos G, Leite SM, Vacanti JP, Langer R. Laminated 3-dimensional biodegradable foams for use in tissue engineering. Biomaterials 1993;14:323–330.
15. Whang K, Healy KE. In: Atlala A, Lanza RP, editors. Methods of Tissue Engineering. San Diego: Acadimic Press; 2002. p 697–704.
16. Brauker JH, Carr-Brendel VE, Martinson LA, Crudele J, Johnston WD, Johnson RC. Revascularization of synthetic membranes directed by membrane microarchitecture. J Biomed Mater Res 1995;29:1517–1524.
17. Kotov NA, Liu YF, Wang SP, Cumming C, Eghtedari M, Vargas G, Motamedi M, Nichols J, Cortiella J. Inverted colloidal crystals as three-dimensional cell scaffolds. Langmuir 2004; 20:7887–7892.
18. Zhang YJ, Wang SP, Eghtedari M, Motamedi M, Kotov NA. Inverted-colloidal-crystal hydrogel matrices as three-dimensional cell scaffolds. Adv Func Mater 2005;15:725–731.
19. Massia SP, Hubbell JA. Covalently attached GRGD on polymer surfaces promotes biospecific adhesion of mammalian-cells. Ann N Y Acad Sci 1990;589:261–270.
20. Barrera DA, Zylstra E, Lansbury PT, Langer R. Synthesis and RGD peptide modification of a new biodegradable copolymer-poly(lactic acid-*co*-lysine). J Am Chem Soc 1993;115:11010–11011.
21. Ratner BD. The engineering of biomaterials exhibiting recognition and specificity. J Mol Recognit 1996;9:617–625.
22. Pradas MM, Ribelles JLG, Aroca AS, Ferrer GG, Anton JS, Pissis P. Porous poly(2-hydroxyethyl acrylate) hydrogels. Polymer 2001;42:4667–4674.
23. Schneider GB, English A, Abraham M, Zaharias R, Stanford C, Keller J. The effect of hydrogel charge density on cell attachment. Biomaterials 2004;25:3023–3028.
24. Ruan WQ, Qian JL, Huang YL, Niu AJ. Synthesis of superabsorbent resin by ultraviolet photo-polymerization. J App Polym Sci 2004;92:1618–1624.
25. Hiroshi Inoue, Tadao Muramatu, Yoshikazu Sasaki, Toshio Ocawaz. Preparation of polyimide powder. J Appl Polym Sci 1996;10:929–933.
26. Mann BK, Schmedlen RH, West JL. Tethered-TGF-b increases extracellular matrix production of vascular smooth muscle cells. Biomaterials 2001;22:439–444.
27. Nguyen Kytai Truong, West JL. Photopolymerizable hydrogels for tissue engineering applications. Biomaterials 2002;23: 4307–4314.
28. Bryant Stephanie J, Bender Ryan J, Durand Kevin L. Anseth Kristi S. Encapsulating chondrocytes in degrading PEG hydrogels with high modulus: Engineering gel structural changes to facilitate cartilaginous tissue production. Biotech Bioengi 2004;86:748–755.
29. Stachowiak AN, Bershteyn A, Tzatzalos E, Irvine DJ. Bioactive hydrogel with an ordered cellular structure combine interconnected macroporosity and robust mechanical properties. Adv Mater 2005;17:399–403.
30. Lu JM, Zhu XL, Zhu J. Microwave radiation solid-state copolymerization in binary maleic anhydride dibenzyl maleate systems. J Appl Polym Sci 1997;66:129–133.
31. Park SA, Shin JW, Yang YI, Kim YK, Park KD, Lee JW, Jo IH, Kim YJ. In vitro study of osteogenic differentiation of bone marrow stromal cells on heat-treated porcine trabecular bone blocks. Biomaterials 2004;25:527–535.
32. Shanbhag S, Wang SP, Kotov NA. Cell distribution profiles in three-dimensional scaffolds with inverted-colloidal-crystal geometry: Modeling and experimental investigations. Small 2005; 1:1208–1214.